Supplementary Information

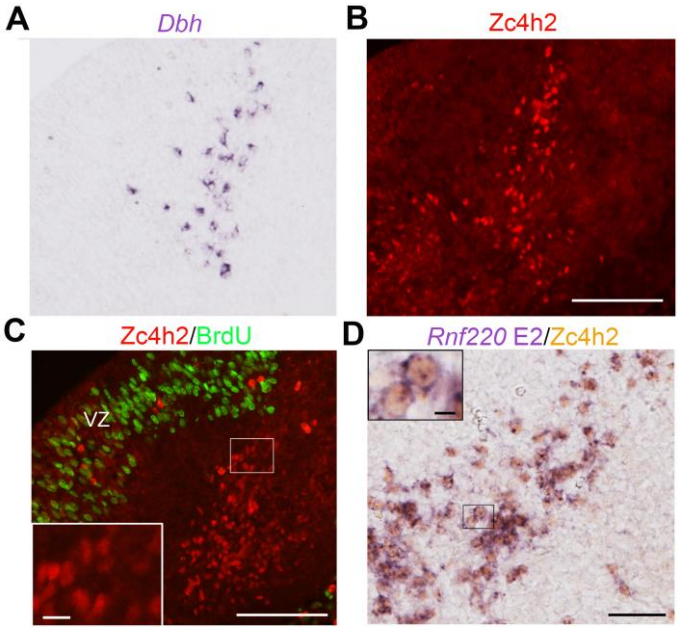

Fig. S1. Expression of Zc4h2 in postmitotic cells of the presumptive LC and co-expression of Rnf220 and Zc4h2 at E11.5.

(A and B) Zc4h2 immunostaining and *Dbh in situ* hybridization are performed in the adjacent sections (B). Scale bar, 100 μm.

(C) Double labeling of Zc4h2 protein and BrdU is performed at E11.5. $Zc4h2^{+}$ cells are located outside BrdU-labeled ventricular zone (VZ). The inset is high magnification of the boxed area. Scale bar, 100 μm and 10 μm in inset.

(D) Double labeling of Zc4h2 protein and *Rnf220* mRNA is performed at E11.5. Scale bar, 100 μm and 10 μm in inset. VZ, ventricular zone.

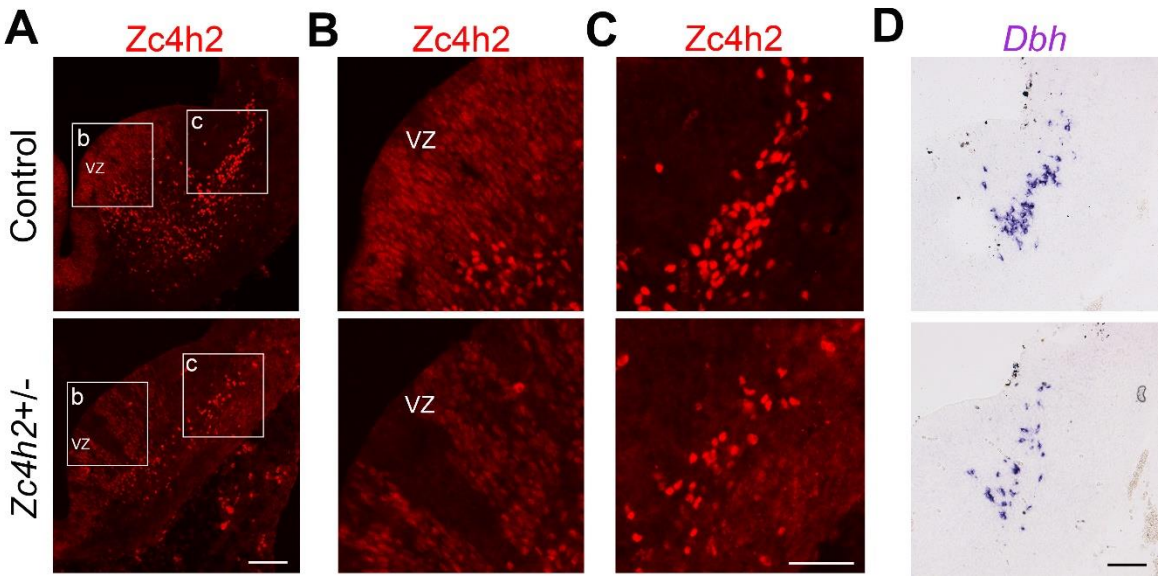

Fig. S2. Abnormal distribution of Zc4h2^{+} cells and a reduction of LC-NA neurons in female *Zc4h2*$^{+/-}$ at E12.5.

(A-C) Immunostaining of Zc4h2 in the ventricular zone (A and B) and the region containing NA neurons (A and C) of female wild-type control and female *Zc4h2* heterozygotes. Weak Zc4h2 immunoreactivity is distributed throughout the VZ in control, but only much fewer cells with weak immunoreactivity are present in the VZ of *Zc4h2* heterozygotes with a patch-like distribution pattern. In the mantle layer outside the VZ, Zc4h2^{+} cells appear to be reduced in number in *Zc4h2* heterozygotes compared with controls. Boxed areas in (A) are enlarged in (B and C). Scale bars, 100 μm in (A), 50 μm in (B and C).

(D) The distribution of NA cells shown by *Dbh* mRNA in the presumptive LC of female control and *Zc4h2* heterozygote, and its number also appeared to be reduced in the heterozygote. Scale bar, 100 μm. VZ, ventricular zone.

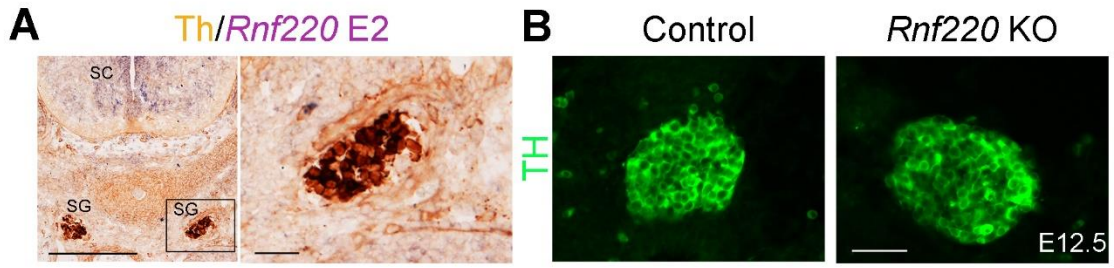

Fig. S3. Expression of Rnf220 in wild-type mice and expression of Th in sympathetic ganglion (SG) in control and *Rnf220* KO mice.

(A) Double labeling of Th protein and *Rnf220* mRNA in wild-type SG at E12.5. Scale bars, 100 μm.

(B) Expression of Th in SG in control and *Rnf220* KO mice at E12.5. Scale bar, 100 μm. SC, spinal cord.

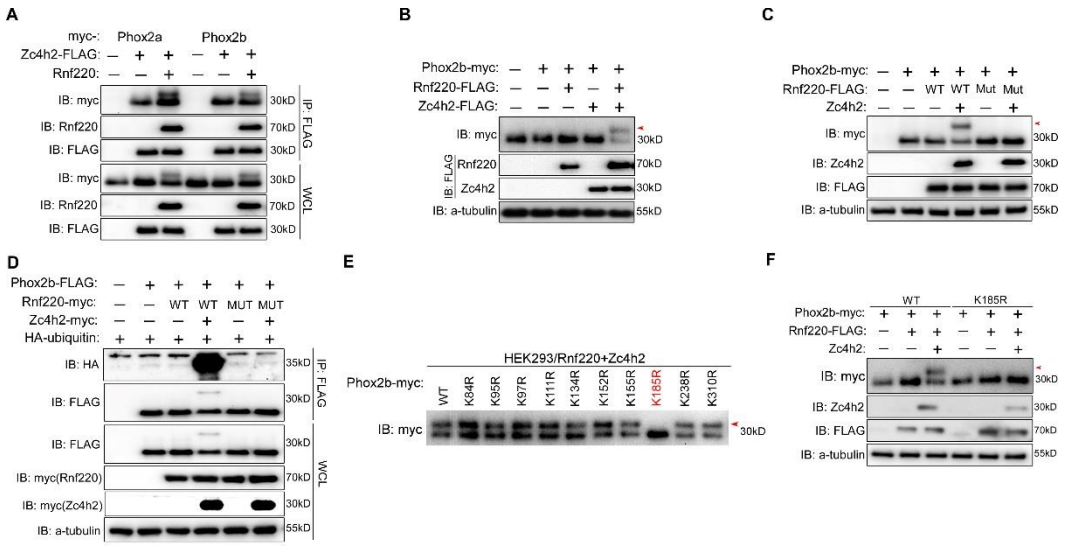

Fig. S4. Rnf220/Zc4h2 complex interacts with and monoubiquitinates Phox2.

(A) Co-immunoprecipitation assays show the interaction between Phox2a/2b and Rnf220/Zc4h2 complex. Phox2a and Phox2b are immunoprecipitated by Zc4h2 in HEK293 cells irrelevant with the presence of Rnf220 (A). The indicated plasmids combinations were transfected into HEK293 cells and the cells were harvested at 48 hrs post transfection for IP analysis. The whole cell lysate and IP samples are analyzed by Western blot. WCL, whole cell lysate; IP, immunoprecipitation.

(B) Western blot data show that a covalent modification band (red arrow) of Phox2b is present only when Rnf220 is co-expressed with Zc4h2 in HEK293 cells.

(C) Western blot data show the presence of the covalent modification band (red arrow) of Phox2b when Zc4h2 is co-expressed with wild-type Rnf220 or its ligase dead mutant in HEK293 cells.

(D) *In vivo* ubiquitination assays in HEK293 cells show that the covalent modification band of Phox2b induced by Rnf220/Zc4h2 is monoubiquitination.

(E) Western blot results show the protein band pattern of Phox2b when the indicated lysines are mutated in the presence of Rnf220 and Zc4h2.

(F) The Phox2b protein monoubiquitination modification (red arrow) induced by Rnf220/Zc4h2 complex is abolished when their indicated lysines are mutated in HEK293 cells.

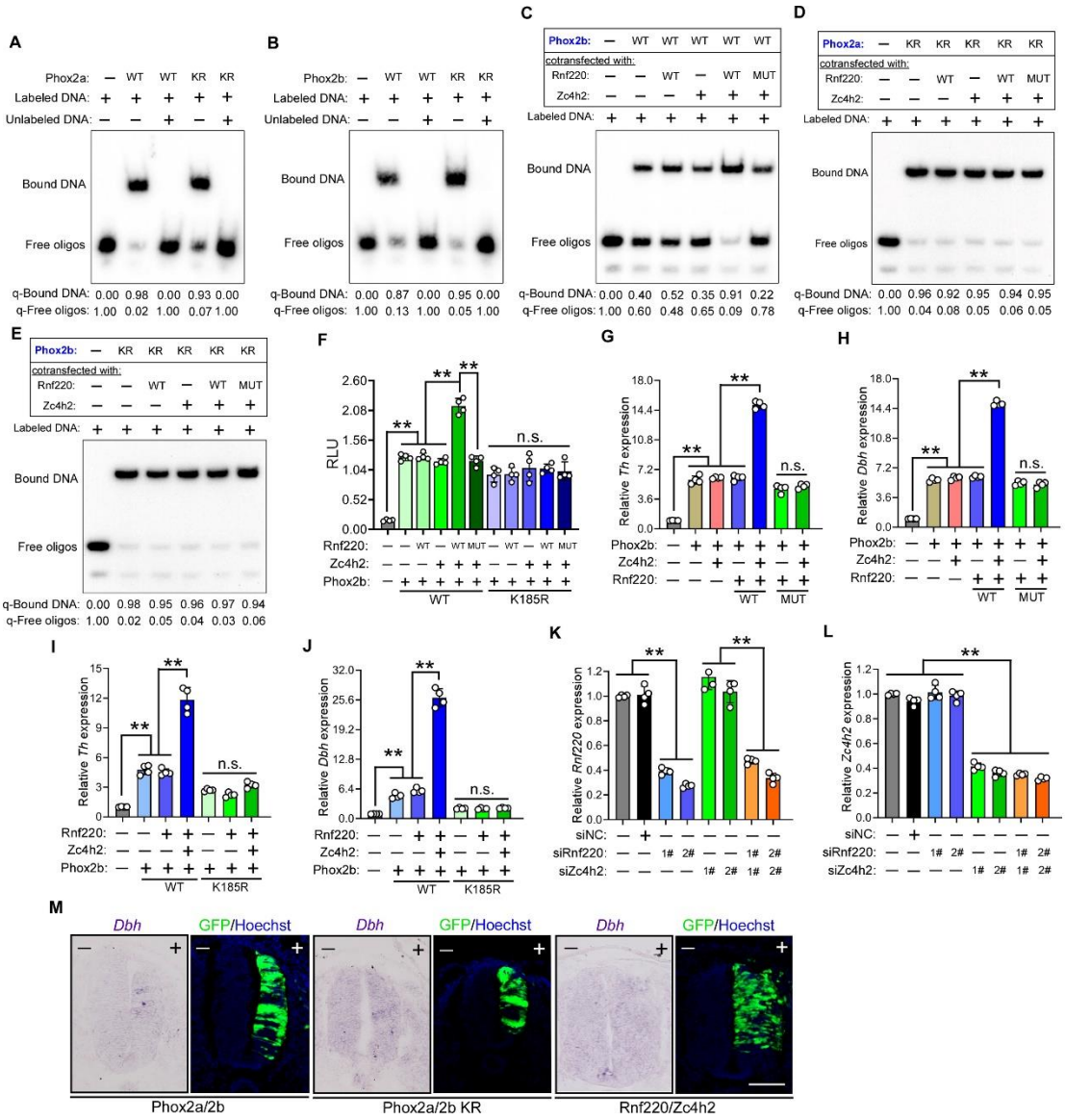

Fig. S5. Phox2 monoubiquitination induced by Rnf220/Zc4h2 complex enhances their DNA binding abilities and transactivites.

(A and B) Gel shift assays show that Phox2a (A) and Phox2b (B) display similar DNA binding abilities.

(C) Gel shift assays show that Phox2b proteins from HEK293 cells with over-expression of wild-type Rnf220/Zc4h2 display enhanced DNA binding abilities.

(D and E) Gel shift assays show that Phox2a (D) and Phox2b (E) KR mutant proteins from HEK293 cells with over-expression of wild-type or ligase dead mutant Rnf220, Zc4h2 or Rnf220/Zc4h2 display similar DNA binding abilities.

(F) Reporter assays show that Phox2b monoubiquitination induced by Rnf220/Zc4h2 complex exhibits enhanced transcriptional activities. Error bars represent S.E.M.

(G and H) Realtime PCR assays show the relative expression levels of *Th* (G) or *Dbh* (H) in the indicated combination of overexpression *Phox2b*, *Zc4h2* and/or *Rnf220* plasmids in CATH.a cells. Error bars represent S.E.M.

(I and J) Realtime PCR assays show the relative expression levels of *Th* (I) and *Dbh* (J) in the indicated combination of over-expression of wild-type Phox2b or its K185R mutant, *Zc4h2* and/or *Rnf220* plasmids is co-expressed in CATH.a cells. Error bars represent S.E.M.

(K and L) Realtime PCR assays show the relative expression levels of *Rnf220* (K) or *Zc4h2* (L) when the indicated siRNAs are transfected in CATH.a cells. The indicated siRNAs combinations were transfected into CATH.a cells and the cells were harvested at 72 hrs post transfection and total RNAs were extracted and subjected to realtime RT-PCR assays. **, $P<0.01$; n.s., no statistical difference, error bars represent S.E.M.

(M) Ectopic expression of *Dbh* was weakly induced in the chick neural tube by over-expression of wild-type Phox2a/2b or their KR mutants but hardly detected in the tube with over-expressing Rnf220/Zc4h2 complex alone. Scale bar, 100 μm.

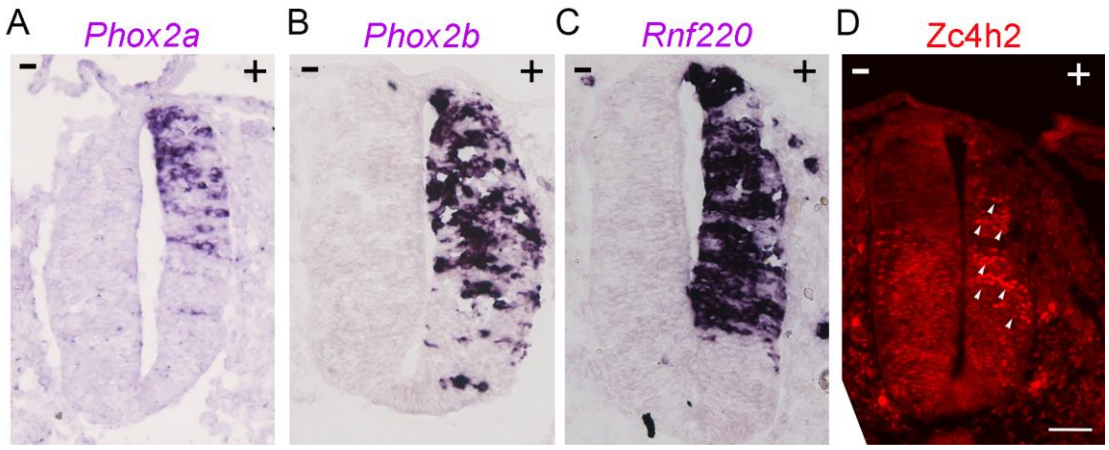

Fig. S6. The ectopic expression of *Phox2a, Phox2b, Rnf220* and Zc4h2 in chick spinal tube after misexpression of wild-type Phox2a/2b with the Rnf220/Zc4h2 complex.

The distribution of *Phox2a* (A), *Phox2b* (B) and *Rnf220* mRNA (C) are revealed by *in situ* hybridization, and Zc4h2 protein (D) is shown by immunofluorescence. Scale bar, 100 μm.